Satellite Observations of the Interplay between Wind and Water Processes in the Great Sahara

Farouk El-Baz

Abstract

Images of the Great Sahara of North Africa obtained by the Advanced Very High Resolution Radiometer (AVHRR), manned missions, and Landsat show regional linear patterns of sand dunes resulting from wind action. These patterns trend southward in the northern part and southwestward in the center of the desert. Radar data from the Spaceborne Imaging Radar (SIR-C) and Radarsat reveal sand- buried courses of palaeo-channels that lead to depressions, which enclose major sand accumulations. Interpretation of these data suggests that the sand originated in the southern part of the Sahara and was carried northward in river courses during past wet climates to be deposited within inland lakes. Prior to the onset of dryness, and the resulting aeolian forms, much of the water would have seeped into the substrate through primary (rock) and/or secondary (fault-induced) porosity to be stored as ground water. Therefore, the exploration for ground water in the Sahara should consider depressions with large accumulations of sand.

Introduction

The interplay between aeolian and fluvial processes in the Great Sahara of North Africa is revealed by the interpretation of satellite images. These include the regional views from the Advanced Very High Resolution Radiometer (AVHRR) instruments onboard the National Oceanic and Atmospheric Administration (NOAA) satellites. Further details are provided by photographs obtained by astronauts on manned missions, images of the Landsat Multi-spectral Scanner (MSS) and Thematic Mapper (TM), as well as radar data from NASA's Spaceborne Imaging Radar (SIR) and Radarsat of the Canadian Space Agency. These data provide unique perspectives that allow the recognition of regional influences on wind action and surface features that result in ground water concentration.

The Great Sahara includes some of the driest regions on the Earth. In its eastern parts, the received solar radiation is capable of evaporating over 200 times the amount of rainfall (Henning and Flohn, 1977). In this desert, precipitation is extremely variable and unpredictable; in some parts it rains only once in 20 to 50 years. This condition necessitates a complete dependence on ground-water resources for human consumption and agricultural activities.

In the past three decades, ground-water levels in the oases depressions throughout the desert have decreased and the known resources are becoming scarce (El-Baz and El-Ashry, 1991). Population growth and attendant food and fiber requirements threaten to exacerbate the situation in the future. Therefore, the need exists to pursue innovative approaches for the location of additional ground-water resources for future use (El-Baz and El-Ashry, 1991).

Although the Sahara is now hyperarid and is subjected to the action of strong winds from the north, geographical, geological, and archaeological evidence indicate that it hosted wetter climates in the past (e.g., Said, 1997). Pre-historic archaeological sites are mainly concentrated along shores of palaeolakes. Surface water during wet climates must have been responsible for the erosion, transportation, and deposition of sand in inland basins (El-Baz, 1998). It follows that these basins would have stored much of the water in the underlying porous sandstone rocks and their fracture zones (Bisson and El-Baz, 1991). During dry conditions that alternated with the wet climate episodes, aeolian activities resulted in the formation of a variety of sand dunes and sand sheets.

The objective of this study was to investigate the causes of localization of large accumulations of sand in the Great Sahara. Interpretation of space-borne images of varying scales provided the necessary indicators of the relationship between sand accumulations and fluvial processes. The latter would have been responsible for the concentration of ground water in the substrate. Therefore, the close relationship between the potential of ground-water occurrence beneath depressions with large accumulations of sand is an important factor in the exploration for this increasingly scarce resource.

Image Dataset

It was important to establish the effectiveness of the major surface processes on a regional scale. Therefore, NOAA satellite data (Table I) were studied to understand the regional setting of the total area of the Great Sahara. The results were compared to, and were found to agree with, maps based on images of Meteosat, the weather satellite of the European Space Agency, which is geostationary over North Africa.

Emphasis in this study was placed on the Western Desert of Egypt, where most of the field confirmations of satellite image interpretations were made. Therefore, it was necessary to establish the setting of large accumulation of sand in that desert. A mosaic of Landsat MSS images (80-m resolution) provided a base for this part of the study. Additional insights were obtained by the study of color photographs obtained by the astronauts of the Gemini (Cortright, 1968) and Apollo-Soyuz (Gifford *et al.*, 1979) missions.

Furthermore, the high spatial resolution of Landsat TM images (30 m) allowed the interpretation of distribution patterns of sand deposits and their relationships to topographic features. These data also served as the base upon which to superimpose radar image strips, and to allow interpretation of zones not covered by these strips (Seto *et al.*, 1997).

Center for Remote Sensing, Boston University, Boston, MA 02215 (farouk@bu.edu).

Photogrammetric Engineering & Remote Sensing
Vol. 66, No. 6, June 2000, pp. 777–782.

0099-1112/00/6606–777$3.00/0

Table 1. Sources of Data Used in the Study

System/Mission	Dataset and Location Information
Apollo-Soyuz	1975 strip of color photographs of the Western Desert of Egypt by a bracket-mounted camera (ASTP-16-1246 to 1257)
Gemini 7	1965 color photographs of eastern Algeria by a hand-held camera (particularly 65-HC-2526)
Landsat MSS	1972–1984 Multi-Spectral Scanner (MSS) image mosaic of the Western Dessert of Egypt (33 scenes)
Landsat TM	1986–1992 Thematic Mapper (TM) image mosaic (ten scenes) of southern Egypt and northern Sudan
NOAA satellite	1995 ten-day (01–10 October) composite AVHRR images; one kilometer resolution (p 127-b2)
Radarsat	1998 Radarsat scene (47-139D; 16344.4332) of area in southeast Libya centered at 22° 16′N; 24° 12′E
SIR-C	1994: (a) Spaceborne Imaging Radar scenes (49) in ten strips within the coverage of the Landsat TM mosaic listed above; (b) one strip of the Kufra Oasis region of southeast Libya

Radar data critical to this study were provided by the imaging radar instrument of the Space Shuttle, which was first flown in November 1981 as SIR-A (Elachi *et al.*, 1982). One image strip covered part of the eastern Sahara in northwestern Sudan. Among the revealed features in that strip were dry courses of wide channels of rivers and streams. One of these rivers measured up to 20 kilometers across; field work indicated that these courses were covered by up to five meters of dry, fine-grained, wind-blown sand (McCauley *et al.*, 1982).

Roth and Elachi (1975) had first theorized that radar can reveal subsurface topography in arid lands and that longer wavelength (L-band) images have the best subsurface imaging abilities. The theory gained widespread recognition after the SIR-A mission. The SIR-B mission encountered problems, but the renamed Spaceborne Imaging Radar (SIR-C) instrument, which was flown on Shuttle missions in April and October 1994, provided other evidence of paleo-channels throughout the Sahara (Schaber *et al.*, 1997; El-Baz and Robinson, 1997). In addition, one Radarsat image revealed a channel in an area in southeastern Libya not covered by SIR-C strips.

Methods Used

This study primarily relied on the visual interpretation of processed images, with field confirmation of observed features, including the following (see Table I):

- Astronaut photographs of the western Sahara (obtained by Gemini 7) and of the eastern Sahara (taken on the Apollo-Soyuz mission). Prints were obtained from the NASA Johnson Space Center, Houston, Texas.
- Landsat MSS images (80-m resolution) of the Western Desert of Egypt were processed and mosaicked. False-color composites were made by combination of bands 4 (green), 5 (red), and 7 (infrared). This combination allowed the depiction of surface details to map the major accumulations of sand in the form of sand sheets and sand dunes.
- Higher resolution Landsat TM images (30-m resolution) were processed using the software package Image Processing Workbench (IPW) and PCI. They were used to overlay SIR-C images of similar resolution (25 m). Only TM band-7 data were used as this band provided enough spectral difference between surface features and geologic units.
- AVHRR data on North Africa were downloaded via ftp from the U.S. Geological Survey EROS Data Center, which holds the Global AVHRR 10-day composite data. Image processing consisted of a linear stretch combined with sharpening using a high pass convolution.
- Used SIR-C data included 49 scenes covering southwestern Egypt and northwestern Sudan. The CEOS-Reader software (obtained from NASA's Jet Propulsion Laboratory) was used to convert the SIR-C data into displayable images. Their processing included histogram equalization, Gaussian and lee filters, and edge filters.
- A Radarsat image of southeastern Libya was directly read from a CD-ROM using PCI Easi/PACE programs. The processing followed the same procedures as that of the SIR-C data.

Observations and Discussion

Prevailing Wind Direction

Regional views of the Great Sahara indicate that surface winds trend in an arcuate pattern that emanates from the direction of the Mediterranean Sea. This is based on the fact that dune lines indicate the direction of the prevailing wind. AVHRR data show that this pattern changes from southward in the northern part of the desert to westward along the borders with the Sahel (Figure 1).

This regional pattern was first suggested for the eastern Sahara based on field mapping by Bagnold (1941). It was also mapped in the rest of the Sahara from Meteosat data by Mainguet (1992; 1995) (Figure 2). Wind-produced erosional scars throughout the desert suggest that this regime was effective during much of the Pleistocene. Sand dune chains in the Western Desert of Egypt prove the consistency of this regime, at least during the past 5,000 years (El-Baz, 1998).

The sand-carrying wind in this desert moves toward the south during most of the year. However, the direction may be locally affected by topographic prominences (Mainguet, 1992). Embabi (1982) measured the rate of motion of dunes in the Kharga depression of the Western Desert of Egypt to vary from 20 m/yr for the large barchans to 100 m/yr for the smallest (1-m high) dunes. Seasonal winds from the south do occur, particularly in mid-Spring, but these are not significant transporters of sand.

Throughout the Sahara, as shown by the global 1-km DEM data and orbital photographs, sand accumulations occur within topographic depressions (e.g., Figure 3). This must be explained in any theory regarding the origin of the sand and the evolution of the dune forms in space and time. Also, the dune sand is composed mostly of well-rounded quartz grains (El-Baz *et al.*, 1979). The exposed rocks to the north of the sand seas are mostly limestones, which could not have been the source of the vast amounts of quartz sand.

These two facts cannot support the conventional view of the origin of the sand by wind erosion and transportation from the north. The majority of the sand appears to have formed by fluvial erosion of sandstone rocks exposed in the southern part of the Sahara. Because areas presently covered by dune sand are topographically low, they must have received sediments from northward flowing stream channels in the geological past. When the conditions of climate changed to dry, the wind from the north sculptured these sand deposits into various dune forms and sand sheets. This suggests that the Great Sahara is a region of sand export; an area of negative sediment balance. The transported sand accumulates in the Sahel belt south of the Sahara; an area of positive sediment balance (Mainguet, 1992).

Sand Dune Patterns

Details of dune patterns in the Sahara were depicted by Gemini photographs (Cortright, 1968), Landsat Multispectral Scanner (MSS) images (Short *et al.*, 1976), and Skylab photographs (McKee *et al.*, 1977). Photographs of the Apollo-Soyuz mission were combined with Landsat MSS images to map the dunes of the eastern Sahara. In the Western Desert of Egypt, which covers an area of 681,000 km^2, over 23 percent of the total area

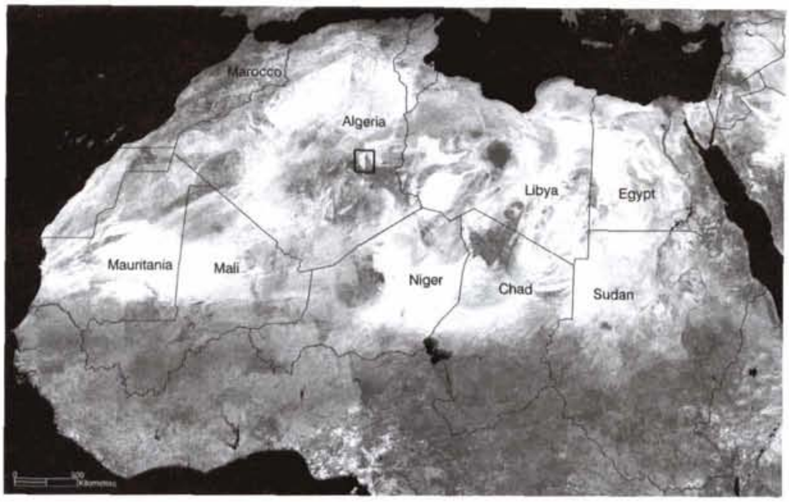

Figure 1. Linear patterns in the Great Sahara as revealed by AVHRR data (courtesy of NOAA). Sandy zones (bright area and lines) trend southward in Egypt, Libya, Sudan, and Chad (eastern Sahara) and southwestward in the western Sahara. (Boxed area in Algeria shows coverage of Figure 3.)

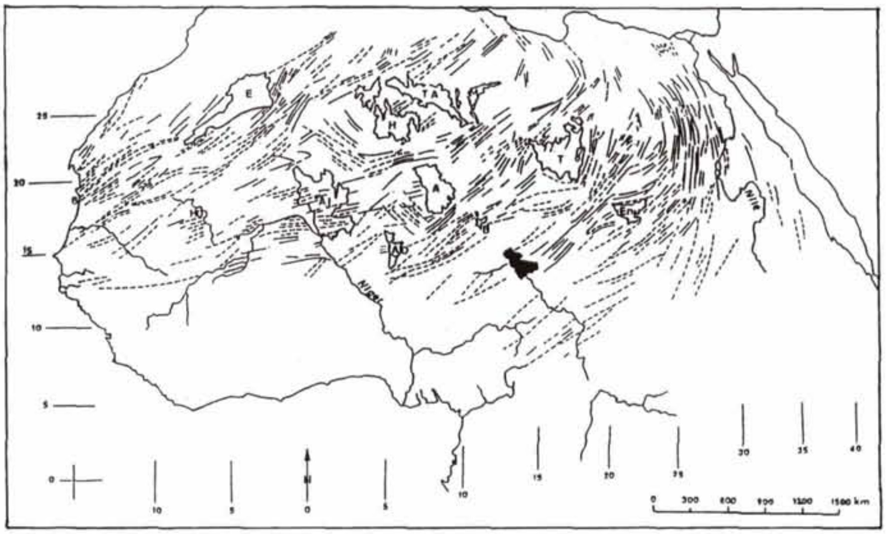

Figure 2. Dune paths in the Great Sahara as interpreted from Meteosat data. Black area is Lake Chad (compare with Figure 1); lettered areas designate mountains (modified after Mainguet (1992) and Mainguet (1995)).

(159,000 km^2) is covered by sand dunes (Gifford *et al.*, 1979). The Great Sand Sea covers 72,000 km^2, where densely packed dunes are confined in a relatively low area in the north and linear forms in the southern part with sand-free corridors (Figure 4).

The linear patterns in the Great Sand Sea (Figure 4) are particularly significant. The long sand bodies were called "whaleback" dunes by Bagnold (1941) who theorized that they grew so large that they no longer could move. Dunes, however, move because individual sand grains are dislodged by the wind, as Bagnold himself noted. Furthermore, cross-sections made into these dunes show that the sand is horizontally laminated rather than curved parallel to dune profiles as in the case of the *seif* dunes that overlie the whaleback forms and the nearby barchan dunes (El-Baz *et al.*, 1979). This suggests that what Bagnold named whaleback dunes are residual sand ridges of horizontally laminated sand, left behind as the wind preferentially eroded the sand in what are seen today as inter-ridge corridors (El-Baz, 1998).

According to conventional geographic and geologic wisdom, "factors controlling the occurrence and morphology of sand deposits are complex; they include the wind direction, strength, and duration; the nature, extent, and rate of erosion at the sediment source; the distance from the source; the grain and fragment size; the underlying and surrounding topography; the nature of the surface (rough or smooth); the amount and type of vegetation; and the amount of rainfall" (Gifford *et al.*, 1979, p. 219).

Figure 3. A 1965 photograph (65-HC-2526) obtained by James Lovell on Gemini 7 showing the basin-bound Tifernine dune field and two smaller dune masses within depressions. The area lies in the Grand Erg Oriental of eastern Algeria, as shown by the box in Figure 1.

Regional views afforded by observations from space allow the realization that the single most important characteristic of areas with high concentrations of sand dunes is their location within topographic depressions (El-Baz, 1998). All the major sand fields of the Great Sahara occur in topographic basins (e.g., Figure 3); in some cases, sand emanates from these low areas as it is driven to higher ground downwind.

El-Baz (1998) proposed that the dune sand originated by fluvial erosion of sandstone rocks such as those of the "Nubian Sandstone" to the south of, or close to, the dune fields of the eastern Sahara. It was, therefore, assumed that the rounding of the grains would have occurred in turbid water as the particulate matter was transported during humid phases in palaeo-rivers and -streams. The sediment load must have been deposited in low areas at the mouths of the palaeo-channels. As the climate became drier, the particulate matter was exposed to the action of wind, which locally mobilized the sand and sculpted it into various dune forms.

Radar-Revealed Palaeo-Channels

SIR-C and Radarsat data unveiled the location of numerous channels of former rivers and streams in the eastern Sahara. The sand cover of these features inhibited their observation in other types of satellite images. The main channels of significance to the present study are discussed below with regard to their occurrence in southwest Egypt, northwest Sudan, and southeast Libya.

Southwest Egypt

SIR-C data depicted drainage channels in the southwestern part of the Western Desert of Egypt. Many of these channels (Figure 5; upper left group of lines) emanate from the Gilf Kebir plateau, a prominent topographic high in southwestern Egypt. The Gilf

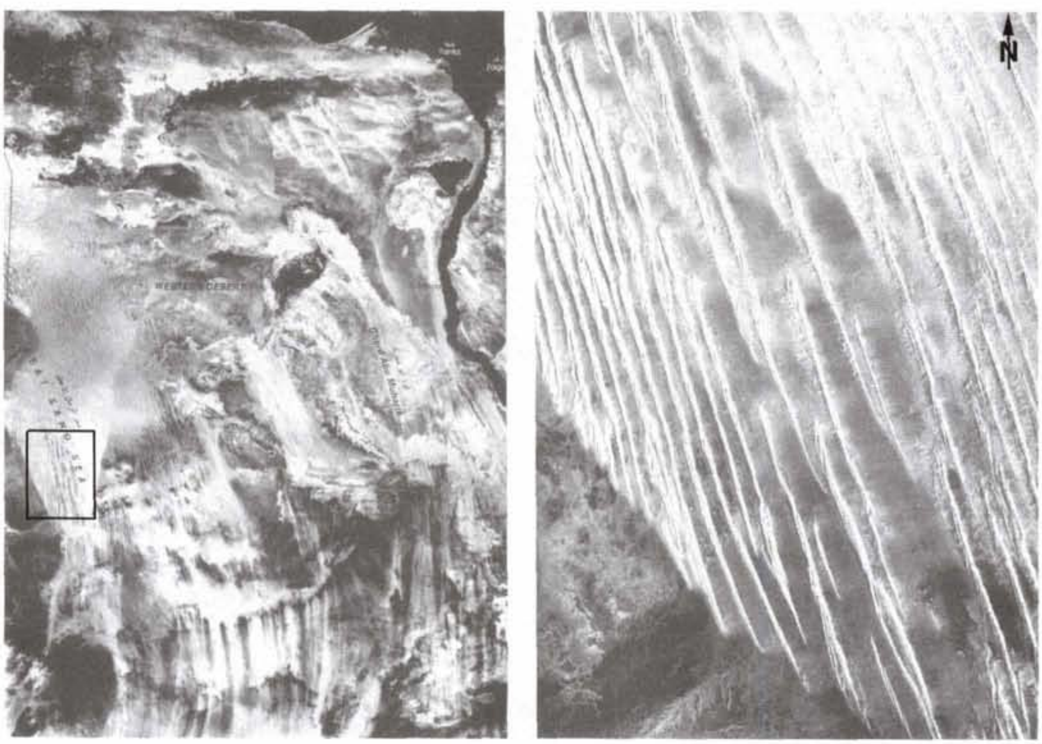

Figure 4. Left, mosaic of Landsat MSS images of the Western Desert of Egypt (700 km wide), with a box around the area of the enlargement to the right (70 km wide), which shows linear sand ridges of the Great Sand Sea with wide inter-ridge corridors.

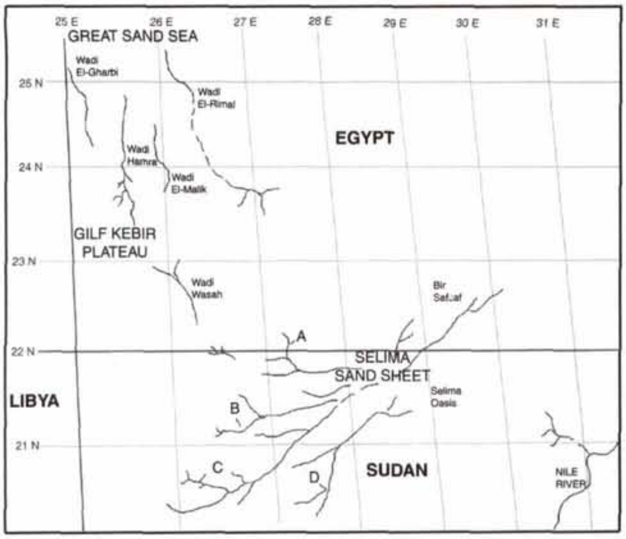

Figure 5. Tracings of radar-revealed channels of former rivers in the eastern part of the Sahara. The group of channels in the upper left leads from the Gilf Kebir plateau in southwestern Egypt (border between Egypt and Libya is at 25° East longitude) to a depression that encloses the Great Sand Sea. The four channels (A through D) in the lower part originate in Sudan and lead to the Great Selima Sand Sheet, which straddles the border between Egypt and Sudan (at 22° North latitude).

is a nearly circular sandstone mass that is centered at approximately 23.5°N, 26°E, with a diameter of 320 kilometers. The plateau is bordered by numerous dry valleys (wadis), indicating that its edges were shaped by fluvial erosion. As Landsat TM images show, the wadis are truncated at the top, which suggests that an upper surface layer of softer sediments had been eroded by both fluvial and aeolian processes. The radar data enhance wadi definition, particularly in the plains. Three major drainage systems-Wadis El-Gharbi, Hamra, and El-Malik-start at the edge of the plateau and trend due north toward the Great Sand Sea. Another, Wadi El-Rimal, starts northeast of the plateau and also trends toward the Great Sand Sea (Figure 5).

Northwest Sudan

Northwestern Sudan is characterized by a vast flat plain over 600 km in diameter. It is known as the Great Selima Sand Sheet after the Selima Oasis, which lies along its southeastern border. This oasis is a prominent location along the Darb El-Arbain (the 40-day track) of camel caravans.

Many drainage lines in the vicinity of the Great Selima Sand Sheet were revealed by SIR-C images with four major lines leading directly to it from the southwest (A through D in Figure 5). The northernmost drainage system A trends due east and measures 150 kilometers in length. The longest wadi system (C) is also very broad and is aligned in a NE-SW direction. Such broad channels usually develop under sheet flood conditions with plentiful surface water.

Several of these broad channels display small braided streams in their floors, as revealed by enlargements of SIR-C data. Braiding usually develops by smaller amounts of surface water, indicating several episodes of water flow. Field observations of trenches dug in May 1998 by a joint team of the Egyptian Geological Survey and the Desert Research Center of Egypt indicate that moisture begins to appear at 25 centimeters depth in the sand cover of shallow channels in the Bir Safsaf region of southern Egypt (Figure 5). This suggests that moisture from occasional rainstorms is carried through, and retained by, the sand fill of the palaeo-channels.

Southeast Libya

Satellite images show that the Kufra Oasis region is the only inhabited area in southeastern Libya. The Oasis had been an important stop along the camel caravan route from Chad northward to the Mediterranean Sea.

The images also show the pattern of circular irrigation farms northeast of the Kufra Oasis. These farms were developed starting in the 1960s by Occidental, as part of a concession to explore for oil. The farms are visible from space due to the contrast (in the visible, near-infra red, and radar data) between the vegetation and the surrounding sandy plain.

SIR-C data reveal the courses of two sand-buried palaeochannels to the southwest of this region (Figure 6). The narrower channel passes through the Kufra Oasis and appears to originate from the direction of the border with Chad. The wider channel is oriented in a NW-SE direction. A Radarsat image of its extension toward the east indicates that it originated from the Gilf Kebir plateau in southwest Egypt. Both the location of the

Figure 6. SIR-C image of the area southwest of the Kufra Oasis, in southeastern Libya, revealing two sand-buried courses of former rivers.

Kufra Oasis and the circular irrigation farms are due, in part, to the presence of these two former rivers.

Implications to Ground Water

The hypothesis made possible by observations from space has far reaching implications to the concentration of ground-water resources in the Great Sahara. Because the sand was transported by paleo-rivers, the depositional inland basins would have received large amounts of fresh water. Much of that water would have seeped into the rocks beneath the sands. Thus, areas that encompass large sand accumulations in the Sahara may be underlain by vast ground-water resources.

Concentration of ground water in topographic basins has particularly been tested in Libya. Because of the encroachment of sea water into the coastal aquifers, Libya had to transport sweet ground water from the southern part of the country to where the population is concentrated along the Mediterranean seacoast. Hundreds of wells were drilled for ground water in five basins: Kufra, Sarir, Sirt, Hamra, and Murzuq (Salem, 1991). The water is transported in a pipeline, which is capable of delivering up to 2,000,000 m^3 per day.

There are indications of a similar hydrogeologic setting in the Western Desert of Egypt. Ground-water exploration in the East Oweinat region of the northern part of the Great Selima Sand Sheet confirmed the presence of resources to support agriculture on 150,000 hectares for 200 years (El-Baz, 1998). Over 80 wells were drilled to a depth of 350 meters; in nearly all cases the water rose in the wells to only 30 meters below the surface. In 1989, this region was assigned to a major land reclamation project by the private sector in Egypt.

Furthermore, two wells near the northern and eastern edges of the Great Sand Sea (Figure 4) proved the presence of vast amounts of water. These wells were drilled south of Siwa Oasis and southwest of Farafra Oasis, respectively, to the depth of 1,200 m in the course of exploring for oil. The two wells penetrated thick sandstone sequences that are saturated with ground water. The water in these two wells fountain under artesian pressure up to 20 m into the air, indicating vast resources at depth (El-Baz, 1998).

Conclusion

Analyses of space images, obtained at varying scales, relate the origin of the sand in the Great Sahara of North Africa to fluvial erosion of the sandstone rocks that are exposed in the southern part of the desert. Interpretation of satellite images suggests the down-gradient transport of the sand grains toward the north in the courses of ancient rivers, which deposited the sand within inland depressions. Much of the water that accumulated in these depressions during wet climate episodes would have seeped through the underlying rocks to be stored as ground water. As dry climates set in, the wind mobilized the sand and shaped it into various dune forms (such as in the Great Sand Sea) and flat plains (such as the Great Selima Sand Sheet). The hypothesis, therefore, implies that sand was born by water and sculpted by the wind. It follows that areas with large accumulations of sand dunes host much ground water beneath the surface. Because similar settings exist in other major deserts of the world, this hypothesis might apply in sandy arid lands worldwide.

Acknowledgments

SIR-C data were obtained from NASA's Jet Propulsion Laboratory. Radarsat data were purchased through a U.S. National Science Foundation grant (INT-9515394). Satellite images were interpreted as part of the UNESCO-sponsored International Geological Correlations Program (IGCP) Project-391. Field work was supported by the Arab League Educational, Cultural and Scientific Organization (ALECSO) in Tunis, Tunisia.

References

Bagnold, R.A., 1941. *The Physics of Blown Sand and Desert Dunes*, Methuen and Co., Ltd., London, 265 p.

Bisson, R.A., and F. El-Baz, 1991. Megawatershed exploration model, *Proceedings of the 23rd International Symposium on Remote Sensing of Environment*, Environmental Research Institute of Michigan, Ann Arbor, 1:247–273.

Cortright, E.M., 1968. *Exploring Space with a Camera*, NASA SP-168, Washington, D.C., 503 p.

Elachi, D., W.E. Brown, J.B. Cimino, T. Dixon, D.L. Evans, J.P. Ford, R.S. Saunders, C. Breed, H. Masursky, J.F. McCauley, G. Schaber, A. Dellwig, A. England, H. MacDonald, P. Martin-Kay, and F. Sabins, 1982. Shuttle imaging radar experiment, *Science*, 218:996–1003.

El-Baz, F., 1998. Sand accumulation and groundwater in the eastern Sahara, *Episodes*, 21(3):147–151.

El-Baz, F., and M.T. El-Ashry, 1991. Ground water for a thirsty earth, *Geotimes*, 36(6):15–18.

El-Baz, F., and C.A. Robinson, 1997. Paleo-channels revealed by SIR-C data in the Western Desert of Egypt: Implications to sand dune accumulations, *Proceedings of the 12th International Conference on Applied Geologic Remote Sensing*, Environmental Research Institute of Michigan, Ann Arbor, 1:469–476.

El-Baz, F., M.H. Slezak, and T.A. Maxwell, 1979. Preliminary analysis of color variations of sand deposits in the Western Desert of Egypt, *Apollo-Soyuz Test Project Summary Science Report: Volume II: Earth Observations and Photography* (F. El-Baz and D.M. Warner, editors), NASA SP-412, Washington, D.C., pp. 237–262.

Embabi, N.S., 1982. Barchans of the Kharga depression, *Desert Landforms of Southwest Egypt: A Basis for Comparison with Mars* (F. El-Baz and T.A. Maxwell, editors), NASA CR-3611, Washington, D.C., pp. 141–155.

Gifford, A.W., D.M. Warner, and F. El-Baz, 1979. Orbital observations of sand distribution in the Western Desert of Egypt, *Apollo-Soyuz Test Project Summary Science Report, Volume II: Earth Observations and Photography* (F. El-Baz and D.M. Warner, editors), NASA SP-412, Washington, D.C., pp. 219–236.

Henning, D., and H. Flohn, 1977. *Climate Aridity Index Map*, U.N. Conference on Desertification, UNEP, Nairobi, Kenya.

Mainguet, M.M., 1992. A global open wind action system: The Sahara and the Sahel, *Geology of the Arab World* (A. Sadek, editor), Cairo University Press, Cairo, Egypt, II, pp. 33–42.

———, 1995. *L'homme et la Secheresse*, Collection Geographie, Mason, Paris, 335 p.

McCauley, J.F., G.G. Schaber, C.S. Breed, M.J. Grolier, C.V. Haynes, B. Issawi, C. Elachi, and R. Blom, 1982. Subsurface valleys and geoarchaeology of the Eastern Sahara revealed by Shuttle radar, *Science*, 218:1004–1020.

McKee, E.D., C.S. Breed, and S.G. Fryberger, 1977. Desert sand seas, *Skylab Explores the Earth*, NASA SP-380, Washington, D.C., pp. 5–47.

Roth, L.E., and C. Elachi, 1975. Coherent electromagnetic losses by scattering from volume inhomogeneities, *IEEE Trans. Antennas and Propagation*, 23:674–675.

Said, R., 1997. The role of the desert in the rise and fall of ancient Egypt, *Sahara*, 9:7–22.

Salem, O., 1991. The Great Man-Made River Project: A partial solution to Libya's future water supply, *Planning for Groundwater Development in Arid and Semi-Arid Regions*, Research Institute for Ground Water, Cairo, Egypt, pp. 221–238.

Schaber, G.C., J.F. McCauley, and C.S. Breed, 1997. The use of multifrequency and polarimetric SIR-C/X-SAR data in geologic studies at Bir Safsaf, Egypt, *Remote Sensing of Environment*, 59:337–363.

Seto, K.C., C.A. Robinson, and F. El-Baz, 1997. Digital image processing of Landsat and SIR-C data to emphasize drainage patterns in southwestern Egypt, *Proceedings of the 12th International Conference on Applied Geologic Remote Sensing*, Environmental Research Institute of Michigan, Ann Arbor, 1:93–100.

Short, N., P.D. Lowman, Jr., S.C. Freden, and W.A. Finch, Jr., 1976. *Mission to Earth: Landsat Views of the World*, NASA SP-360, Washington, D.C., 459 p.